

Journal of
Mechanics of
Materials and Structures

**PROTECTION PERFORMANCE OF DOUBLE-LAYERED METAL
SHIELDS AGAINST PROJECTILE IMPACT**

Xiaoqing Teng, Sumita Dey, Tore Børvik and Tomasz Wierzbicki

Volume 2, N° 7

September 2007

PROTECTION PERFORMANCE OF DOUBLE-LAYERED METAL SHIELDS AGAINST PROJECTILE IMPACT

XIAOQING TENG, SUMITA DEY, TORE BØRVIK AND TOMASZ WIERZBICKI

This paper critically evaluates the protection performance of double-layered shields against projectile impact at the subordnance velocity using finite element methods. Four types of projectiles of different weight and nose shape are considered, representing various fragments generated from Improvised Explosive Devices (IEDs). It is found that the double-layer configuration is able to improve the ballistic resistance by 8.0%–25.0% for the flat-nose projectile, compared to the monolithic plate of the same weight. The upgrade is due to the transition of the failure mode from less energy dissipating shear plugging to more energy dissipating tensile tearing. Under impact by the conical-nose projectile, the double-layered target is almost as capable as the monolithic plate. The present research helps resolve the long outstanding issue of the protection effectiveness of the double-layer configuration.

1. Introduction

Optimization design of metal shields for protection against projectile impact has long been of interest in military and civilian applications. As a potential improvement over monolithic plates, a multiple layer configuration that consists of several parallel plates has been proposed. Compared with numerous experimental, numerical, and theoretical investigations on the impact failure response of single-layered shields, only limited studies on the performance of multilayered targets were reported in the open literature.

Marom and Bodner [1979] investigated experimentally and theoretically the perforation behavior of multilayered beams under impact by a spherical-nose bullet projectile. They concluded that the multilayered structures were more effective than the uniform beams of the same weight. Corran et al. [1983b; 1983a] found from a series of impact tests that a double-, triple-layered target would be superior in the ballistic resistance than a monolithic shield if the total thickness exceeded a critical value. An opposite conclusion was obtained by Radin and Goldsmith [1988]. They performed normal impact tests of a blunt-nose and a conical-nose projectile on multilayered plates. The ballistic limits of the single-layered plates were always higher than those of the multiple-layered targets for both types of projectiles. Note that the thickness of the targets tested by Radin and Goldsmith ranges from 1.6 mm to 6.4 mm. Almohandes et al. [1996] confirmed this finding by conducting an extensive experimental study on steel shields of various configurations struck by standard 7.62 mm bullet projectiles. An experimental and numerical study on the protection effectiveness of double-layered steel shields was recently executed by Dey et al. [2007] and Børvik et al. [2006]. It was found that in the case of the blunt-nose projectile the ballistic limits can be improved by more than 30% by adopting the double layer configuration.

Keywords: double layer, projectile, perforation, fragments.

Partial support of this work by the Army Research Office (ARO) under Grant W911NF-06-1-0232 is gratefully acknowledged.

Besides experimental and numerical studies, several analytical models were also developed for the estimation of the ballistic resistance of multilayered shields. For example, Ben-Dor et al. [1998; 2006] studied effects of the spacing between plates on the ballistic limits. They concluded that increasing the spacing produced no significant change. Elek et al. [2005] extended the penetration model developed by Liss et al. [1983] to the case with multilayered targets. The theoretical solutions indicate that a monolithic target has greater ballistic resistance than a multilayered shield of the same thickness. Liang et al. [2005] proposed a simple theoretical model for the shear plugging process of multilayered shields.

It appears from the above literature review that the protection effectiveness of multilayered shields remains a subject of controversy. This inconsistency poses an interesting question: Under what kind of projectile impact would a double-layered shield be superior in the ballistic limit than a monolithic plate of the same weight?

Different failure modes may develop in a single target due to changing impact conditions [Børvik et al. 2002a; 2002b; Teng and Wierzbicki 2005a; 2005b]. If we could promote a failure mode with higher energy absorption, the ballistic resistance of a shield can be significantly improved. By replacing a monolithic plate with a double-, multilayered shield, the bending flexibility can be increased allowing a target to undergo considerable deformation before fracture. The objective of the present paper is to evaluate the performance of the double layer configuration against projectile impact.

A variety of projectiles including heavy fragments generated from IEDs and light bullet hard-core projectiles may be encountered in practical applications. An armor shield would behave differently under the impact of different projectiles. To thoroughly investigate the protection effectiveness of a target four types of projectiles of different weight and nose shape are considered in this study.

The introduction of the double layer configuration brings into the analysis three additional important parameters: spacing, material combination, and thickness ratio between two plates. For simplicity, the present paper assumes that the two plates are identical to each other, that is, the two plates are made of the same metal and are of the same thickness. We focus on effects of the spacing between the two plates. The advantage of using two different grades of steels for the two layers is a subject of a separate study.

Even with this simplification, an extensive parametric study has to be conducted to determine the ballistic limit of each projectile-target system. Such an approach would not be affordable by means of tests alone. As an alternative to determine experimentally the V_{50} , leading commercial finite element codes such as ABAQUS/Explicit and LS-DYNA are able to fulfill this task provided that they are equipped with a suitable fracture model. In this study, ABAQUS/Explicit is used to simulate all perforation processes. Numerical modeling provides an insight into failure mechanisms and may help reduce the number of necessary tests. Finally, the paper concludes by pointing out the advantages of the double layer configuration over the monolithic plate.

2. Problem description

2.1. Computational models. We consider three types of metal shields including a monolithic plate, a double-layered shield with the plates initially in contact, and a double-layered shield with the plates spaced, as shown in Figure 1. Monolithic plates are commonly used in practice for armor protection, and this case will be taken as a reference in the present study. Two identical plates are defined in the double layer configuration. The plates interact with each other through compression but not tension.

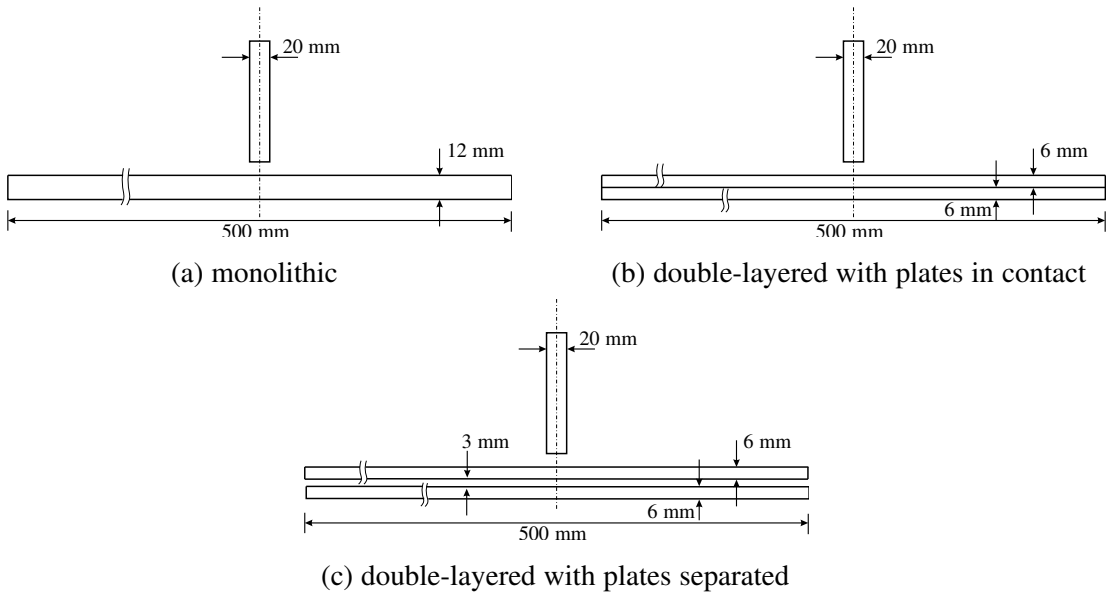


Figure 1. Three types of shields considered in this work.

Limited shear stress due to friction can also be transmitted between the two plates. The shields are of circular shape with the same diameter of 500 mm and the same total thickness of 12 mm. These geometrical dimensions were taken from the impact tests on the monolithic plates conducted by Børvik et al. [2002b]. In the third type of shields the spacing between the two plates is 3 mm, which is 25% of the total thickness still allowing the two plates to interact with each other.

Two major types of armor-piercing projectiles are often encountered in battles: 7.62 mm armor-piercing (AP) bullets from rifles or machine guns and fragments generated from IEDs. The ball rounds have mass usually of the order of 10 g and are of ogival-nose shape. By contrast, fragments may come in a variety of weight and configurations. To design light armor shields for protection against fragments, U.S. military standard MIL-P-46593A prescribes three types of Fragment Simulating Projectiles (FSPs) with mass of 44 g, 207 g, and 830 g, respectively [DoD 1962]. All these FSPs are of cylindrical shape and chisel-nose. In this paper four types of cylindrical projectiles are considered; see Figure 2. We have defined for them two masses of different orders of magnitude: 200 g and 10 g. The heavy projectiles describe typical IED fragments. At the same time, two types of impactor noses were introduced: flat-nose and conical-nose, which denote two limiting cases. The light, conical-nose projectile coarsely represents a 7.62 mm AP round.

With different combinations of the three metal shields and the four projectiles, there are a total of twelve impact cases in this research. For each case, the initial impact velocity of the projectiles varies in a wide range and the ballistic limit is found when the exit (residual) velocity becomes zero. The protection performance of the three metal shields is evaluated by comparing their ballistic limits.

A two-dimensional finite element model was generated for each projectile-target plate system. The target plates were modeled using four-noded axisymmetric elements with reduced integration (CAX4R). The *relax stiffness* option of the integral viscoelastic form was defined to control possible hourglass

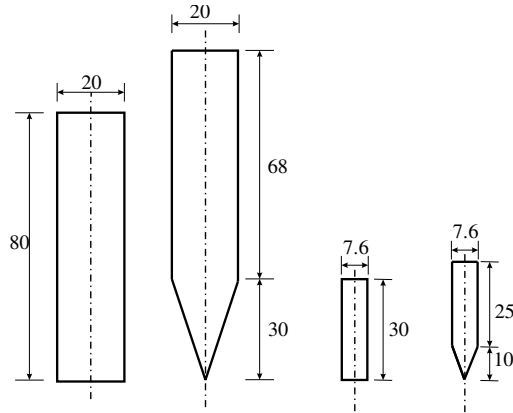


Figure 2. Dimensions of four cylindrical projectiles considered in this work (unit: mm).

deformation for this type of elements. [Figure 3](#) shows a finite element model for the double-layered shield with the plates spaced. The impacted zone below the projectile was discretized with 120 square elements through the thickness, that is, the minimum element size is 0.1×0.1 mm. An early study on mesh size effects indicates that numerical simulations based on such an element size correlate well with experimental results [[Teng and Wierzbicki 2005a](#)]. The projectiles were assumed to be undeformable and were simply represented by rigid surfaces in the simulations. The introduction of this assumption may underestimate the ballistic limits of the targets. In reality, projectiles would absorb a certain amount of the kinetic energy and may break into several pieces under shock wave loading [[Børvik et al. 2003](#)]. Such complex projectile behaviors are not taken into account in this numerical investigation.

To correctly simulate a whole perforation process, one has to carefully define contact conditions between any two bodies that may interact with each other. For the monolithic shield, the kinematic contact constraint was prescribed between the projectile and the impacted zone of the target. The problem becomes much more complex for the case with the double-layered shield. The projectile may sequentially

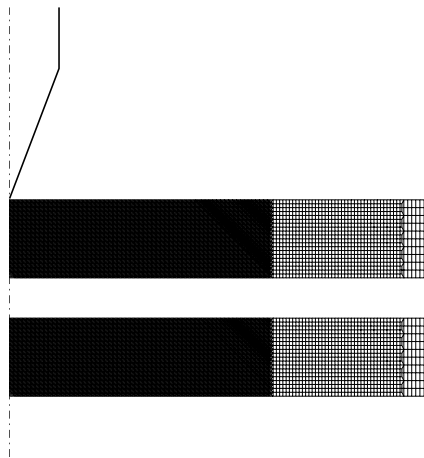


Figure 3. Finite element model of the impacted zone of a double-layered shield with plates spaced, impacted by a conical-nose projectile.

get into contact with the two plates and at the same time the two plates will act on each other. Three contact constraints need to be specified. Two kinematic contact constraints were defined between the projectile and the two target plates, respectively. The penalty contact constraint was prescribed between the two plates. A constant frictional coefficient of 0.1 was defined on all the possible contact interfaces.

2.2. Plasticity and fracture models for Weldox 460 E steel. The target plates were assumed to be made of Weldox 460 E steel. Weldox is the brand name of a class of rolled steels manufactured by SSAB, Sweden. This class of steel is of high strength and at the same time of outstanding ductility. Børvik et al. [2001; 2005] conducted a series of tensile tests on round bars to characterize mechanical properties of Weldox 460 E steel. The material constitutive model proposed by [Johnson and Cook 1983] was selected to describe the plastic behaviors of the steel under dynamic loading. The hardening rule including effects of strain rates and elevated temperature is defined by

$$\bar{\sigma} = [A + B\bar{\epsilon}_{\text{pl}}^n] \left[1 + C \ln \left(\frac{\dot{\bar{\epsilon}}_{\text{pl}}}{\dot{\bar{\epsilon}}_0} \right) \right] \left[1 - \left(\frac{T - T_0}{T_m - T_0} \right)^m \right],$$

where $\bar{\sigma}$ is the von Mises stress, $\bar{\epsilon}_{\text{pl}}$ is the effective plastic strain, A , B , n , C , and m are five material constants to be calibrated from tests, $\dot{\bar{\epsilon}}_{\text{pl}}$ and $\dot{\bar{\epsilon}}_0$ are the current and reference strain rate, T_m and T_0 are the melting and room temperature. Below we list relevant material constants for Weldox 460 E steel:

$$\begin{aligned} E &= 200 \text{ GPa}, & \nu &= 0.33, & \rho &= 7850 \text{ kg/m}^3, & \dot{\bar{\epsilon}}_0 &= 5.00 \times 10^{-4} \text{ s}^{-1}, & C &= 0.0123, \\ c_v &= 452 \text{ J/kg K}, & T_m &= 1800 \text{ K}, & T_0 &= 293 \text{ K}, & m &= 0.94, & A &= 490 \text{ MPa}, \\ B &= 383 \text{ MPa}, & n &= 0.45, & D_1 &= 0.0705, & D_2 &= 1.732, & D_3 &= -0.54. \end{aligned}$$

A ductile fracture model formulated in the space of the stress triaxiality and the effective plastic strain was adopted to predict the material failure. Such a fracture criterion can be written most generally as

$$D = \int_0^{\bar{\epsilon}_{\text{pl}}} \frac{1}{\bar{\epsilon}_{\text{f}}(\eta)} d\bar{\epsilon}_{\text{pl}},$$

where D is the damage indicator, $\bar{\epsilon}_{\text{f}}$ is the effective plastic strain to fracture, and η is the stress triaxiality defined by the ratio of the mean stress σ_m to the equivalent stress. A material point is said to fail when D reaches or exceeds the unity, that is, $D \geq 1.0$. This type of fracture model was first suggested by Johnson and Cook [1985], and has been incorporated into many leading commercial finite element codes. The effective fracture strain as a function of the stress triaxiality has to be determined from tests. Johnson and Cook [1985] suggested an exponential relationship $\bar{\epsilon}_{\text{f}} = D_1 + D_2 \exp(D_3\eta)$, where D_1 , D_2 , and D_3 are three material coefficients. Based on a series of tensile tests on notched and unnotched round bars, Børvik et al. [2001; 2005] obtained the following data for Weldox 460 E steel: $D_1 = 0.0705$, $D_2 = 1.732$, and $D_3 = -0.54$. In many practical applications Johnson–Cook fracture loci calibrated from tensile tests were often extrapolated to the range of negative stress triaxialities. In such a way, the ductility of materials under compression may be underestimated. Here, the Johnson–Cook fracture locus was modified by incorporating a cut-off value for the negative stress triaxiality at $-1/3$; see Figure 4. The concept of the cut-off value was first introduced by Bao and Wierzbicki [2005] to account for the sharp increase of the ductility of materials under compression. The cut-off value has a critical effect on the reconstruction of various fracture patterns encountered in high velocity impact tests. This has been

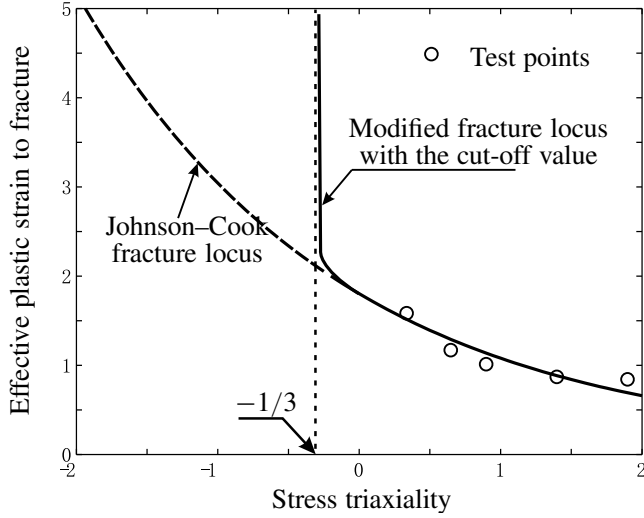


Figure 4. Fracture loci for Weldox 460 E steel.

successfully demonstrated in [Teng and Wierzbicki 2005b; Teng et al. 2005] for a number of impact problems.

Note, that the present fracture criterion is uncoupled with the material plasticity model. An element fails as soon as its damage indicator reaches the critical value. Failed elements completely lose their load-carrying capability and are removed from the rest of the calculation.

3. Perforation response of three types of shields

3.1. Heavy flat-nose projectile. The first striker considered is the heavy, flat-nose projectile, which represents a fragment generated from IEDs. Shear plugging is the predominant failure mode for the monolithic target under normal impact by this projectile. Its sharp corner often induces crack formation on the proximal surface. As the crack propagates through the plate thickness, the whole impacted zone beneath the projectile is ejected as a plug. Figure 5 shows a typical fracture process of the monolithic shield captured by the present numerical simulation at $V_0 = 285.4$ m/s. It can be observed that the target

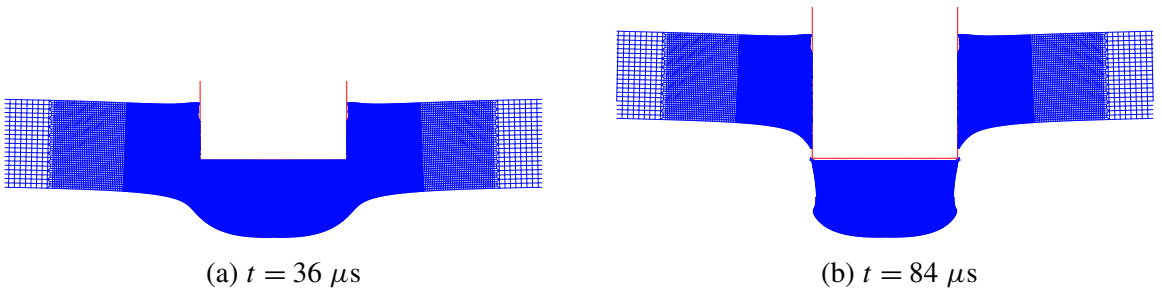


Figure 5. Shear plugging process of monolithic plate impacted by a heavy, flat-nose projectile at $V_0 = 285.4$ m/s.

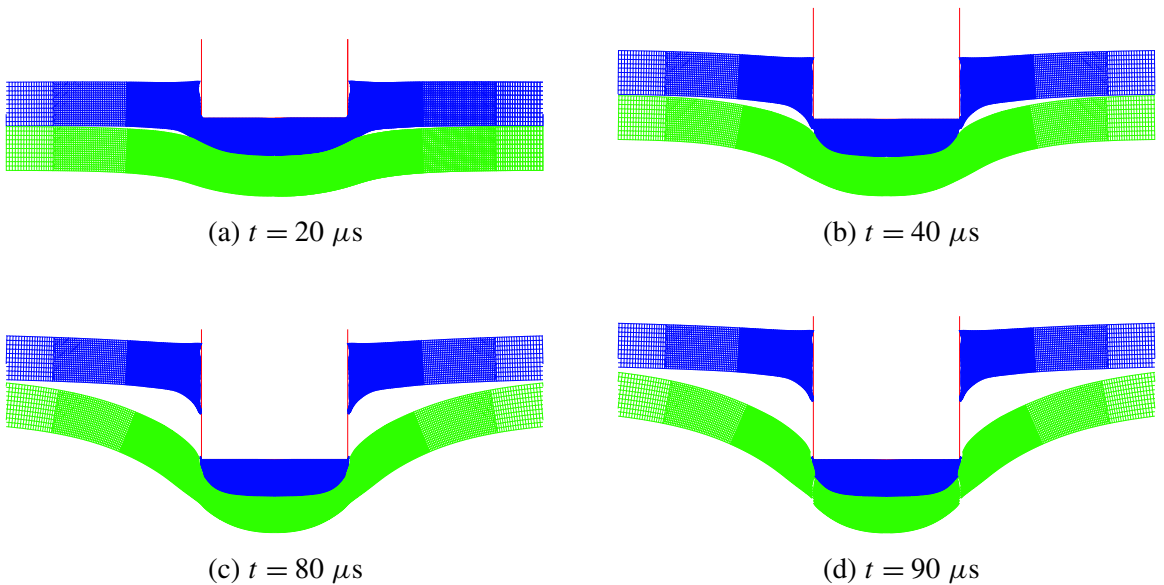


Figure 6. Perforation of double-layered shield with plates in contact impacted by a heavy, flat-nose projectile at $V_0 = 285.4$ m/s.

plate undergoes insignificant global deformation even at the impact velocity near the ballistic limit. Some of the impact velocities in the numerical simulations were selected to be identical to those in the impact tests performed by Børvik et al. [2002b]. In this way, one would be able to directly verify the correctness of the numerical results.

For the double-layered shield with the plates in contact, the upper plate tends to fail by shear plugging and the plastic deformation is localized in the impacted zone. This is similar to the monolithic target. However, the deformation region of the lower plate extends well beyond the impacted zone. Thinning before fracture can be clearly observed in the lower plate; see Figure 6. Unlike the monolithic plate in which one single crack continuously grows through the whole thickness, two separate cracks have to be formed, one for each plate in the double-layered shields. In general, crack initiation requires more energy dissipation than crack propagation.

The failure process of the double-layered shield with the plates spaced is illustrated in Figure 7. It appears that the upper plate suffers considerable bending deformation before contacting with the lower one. At the same time, one can see that the lower plate experiences deep necking and fails mainly by tensile tearing.

The transition of the failure mode from shear plugging in the monolithic plate to tensile tearing in the double-layered shield is accompanied with a large increase in plastic energy dissipation, particularly in the lower plate. Under the same impact condition, tensile tearing usually involves a larger plastically deformed area than shear plugging. Figure 8 shows the time evolution of the plastic energy dissipation of the upper and lower plates among the three types of shields. For comparison, for the monolithic plate, the plastic energy for the upper and lower half was output separately. The plastic energy absorbed by the

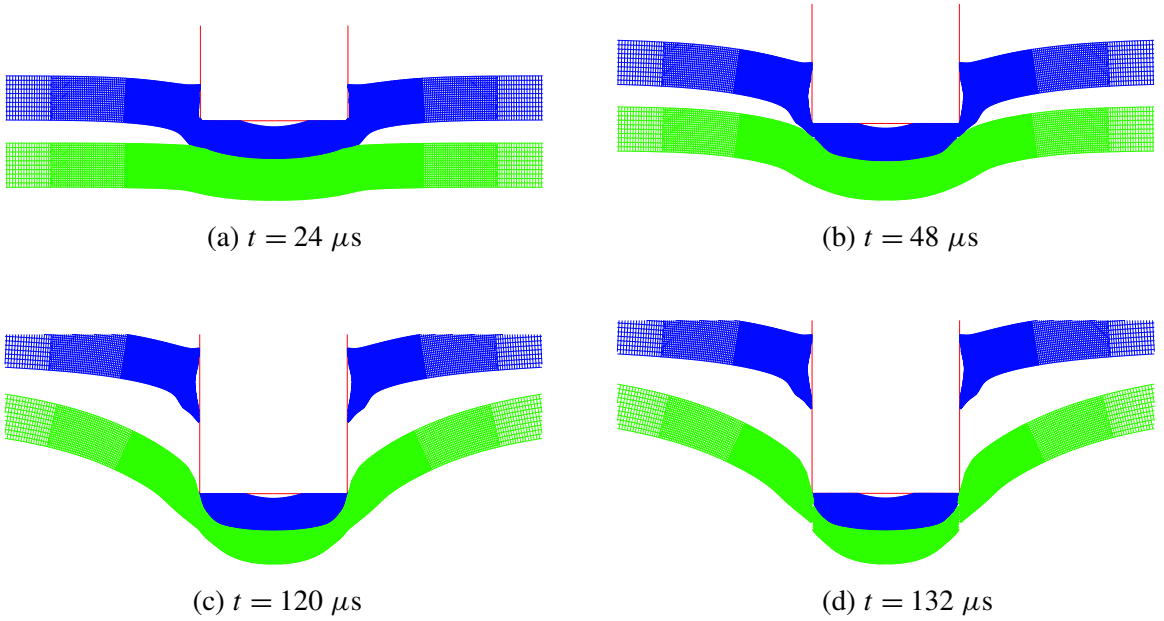


Figure 7. Perforation of double-layered shield with plates spaced impacted by a heavy, flat-nose projectile at $V_0 = 285.4$ m/s.

lower plate of the double-layered shield with the plates spaced is almost twice as large as that absorbed by the lower part of the monolithic target.

Large energy dissipation leads to low residual velocities of the projectile in the case of double-layered shields. Figure 9 shows plots of the residual velocity of the projectile versus the initial impact velocity

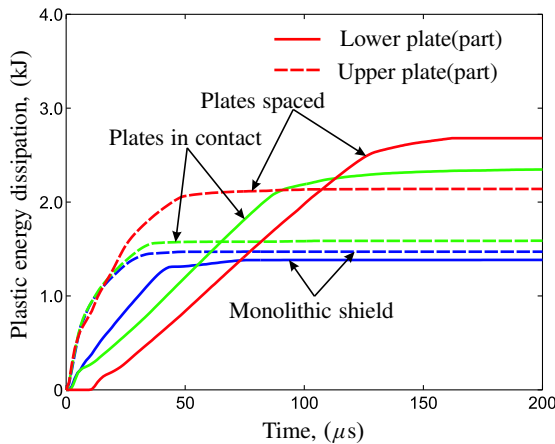


Figure 8. Time history of plastic energy dissipation of three shields at $V_0 = 285.4$ m/s.

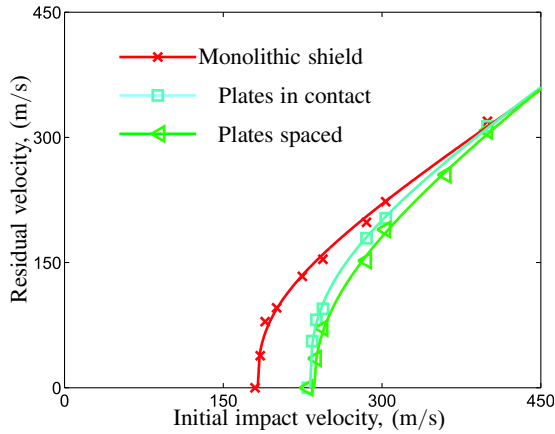


Figure 9. Initial impact velocity vs. residual velocity for three shields impacted by a heavy, flat-nose projectile.

among the three cases. As the impact velocity approaches the ballistic limit, the double-layered shields become superior in resisting perforation to the monolithic plate. Table 1 lists the ballistic limits of the three types of metal shields under impact by the heavy, flat-nose projectile. The ballistic limit of the metal shield is improved by about 25% by replacing the monolithic plate with the double-layered shields of the same total thickness. This finding is confirmed by the impact tests recently conducted by Dey et al. [2007]. They observed that the double layer configuration was able to increase the ballistic resistance by about 30%. The present numerical prediction is also consistent qualitatively with Corran et al.’s experimental results [1983b; 1983a], but contradicts test outcomes of Radin and Goldsmith [1988]. As Corran et al. [1983b; 1983a] pointed out, the double layer configuration would become more effective than the monolithic one as the total thickness exceeded a critical value. Note that the thickness of the targets studied by Radin and Goldsmith ranges from 1.6 mm to 6.4 mm, which is much smaller than in the current study.

It can be seen from Figure 9 that for the double-layered shields an increase in the spacing between the two plates slightly improves the ballistic resistance. This conclusion is contrary to the experimental results obtained by Marom and Bodner [1979], who found that the beams in contact always have higher ballistic limits than the beams spaced. It should be noted, however, that in their study the beams were so widely separated that there was essentially no interaction between them during the whole perforation process. In the present case, the two plates in the double-layered shields strongly interact with one another. This inconsistency indicates that there may exist an optimal spacing for the double-layered shield.

Monolithic plate	Double-layered shield	
	plates in contact	plates spaced
186.1 (1.00)	232.0 (1.25)	236.0 (1.27)

Table 1. Ballistic limits under the impact of a heavy, flat-nose projectile (unit: m/s).

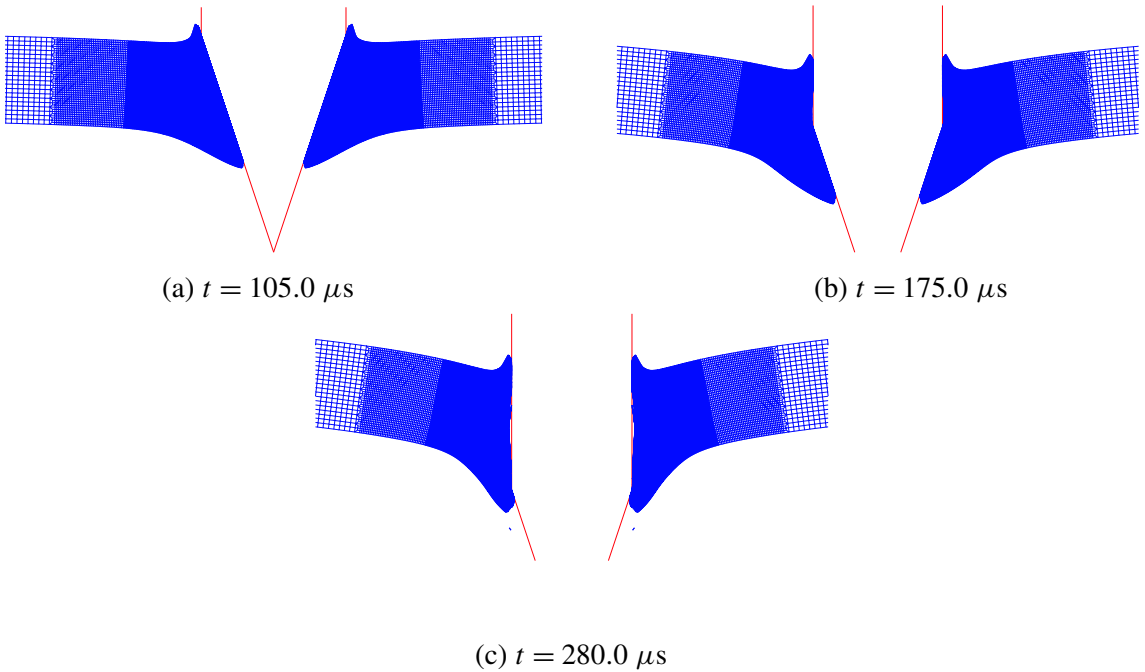


Figure 10. Perforation of monolithic shield impacted by a heavy, conical-nose projectile at $V_0 = 317.9$ m/s.

3.2. Heavy conical-nose projectile. In the preceding section the surface contact between the fragment projectile and the target was assumed. It is more likely that the sharp corner of a fragment would first pierce a metal shield in real situations. This type of perforation scenario is considered here by introducing the heavy, conical-nose projectile. Figures 10–12 illustrate the failure processes of the three types of shields under normal impact by the conical-nose projectile. In the second case the lower plate undergoes larger bending deformation than the upper plate. This leads to a clear separation between the two plates, which are initially in close contact. It can also be seen that in the three cases the materials in the impacted zone are pushed aside as the projectile penetrates through the thickness. There is no clear sign of crack formation and propagation. All the target plates fail by ductile hole enlargement, independent of the configuration and the impact velocity. Hence, the introduction of the double-layered configuration does not induce the transition of the failure mode for the conical-nose projectile. This is in contrast to the preceding case with the flat-nose projectile.

Plots of the initial impact velocity versus the residual velocity for the three types of metal shields are shown in Figure 13. The predicted residual velocities for the double-layered shields are always higher than those for the monolithic plate. Since neither large shear nor tensile stresses can be transferred between the two plates, the shear resistance of the double-layered shields is weakened. This leads to an 8% decrease in the ballistic limits compared to the monolithic plate; see Table 2. This conclusion is qualitatively in agreement with the experimental results obtained by Radin and Goldsmith [1988], Almohandes et al. [1996], and Dey et al. [2007].

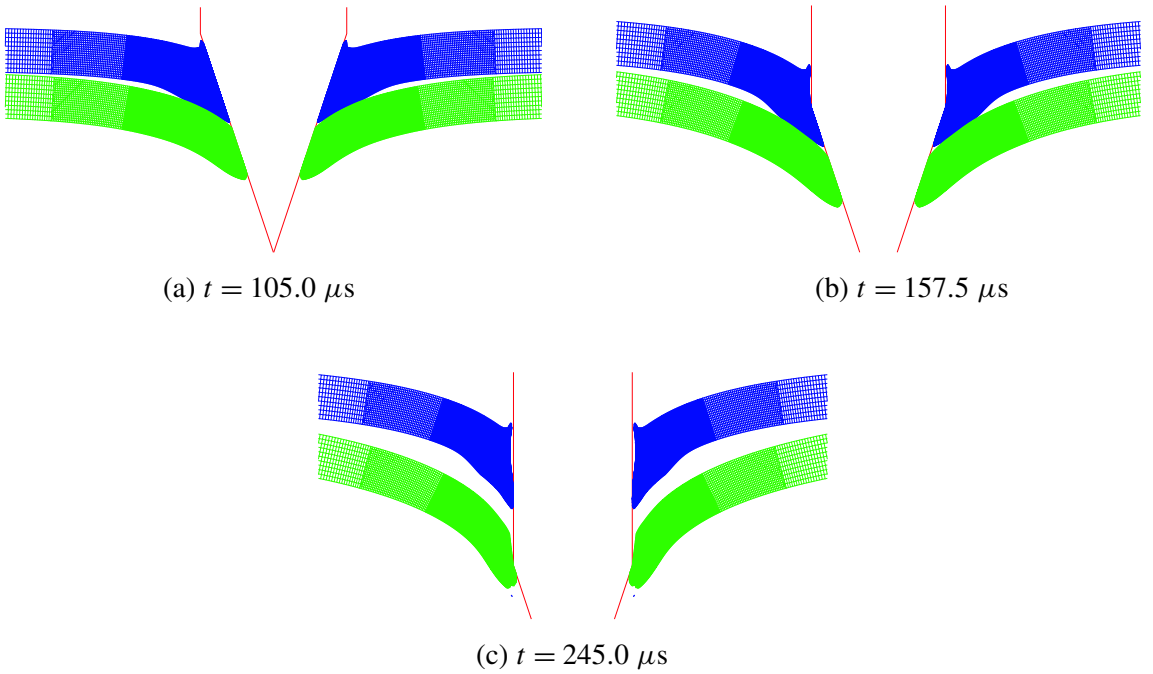


Figure 11. Perforation of double-layered shield with plates in contact impacted by a heavy, conical-nose projectile at $V_0 = 317.9 \text{ m/s}$.

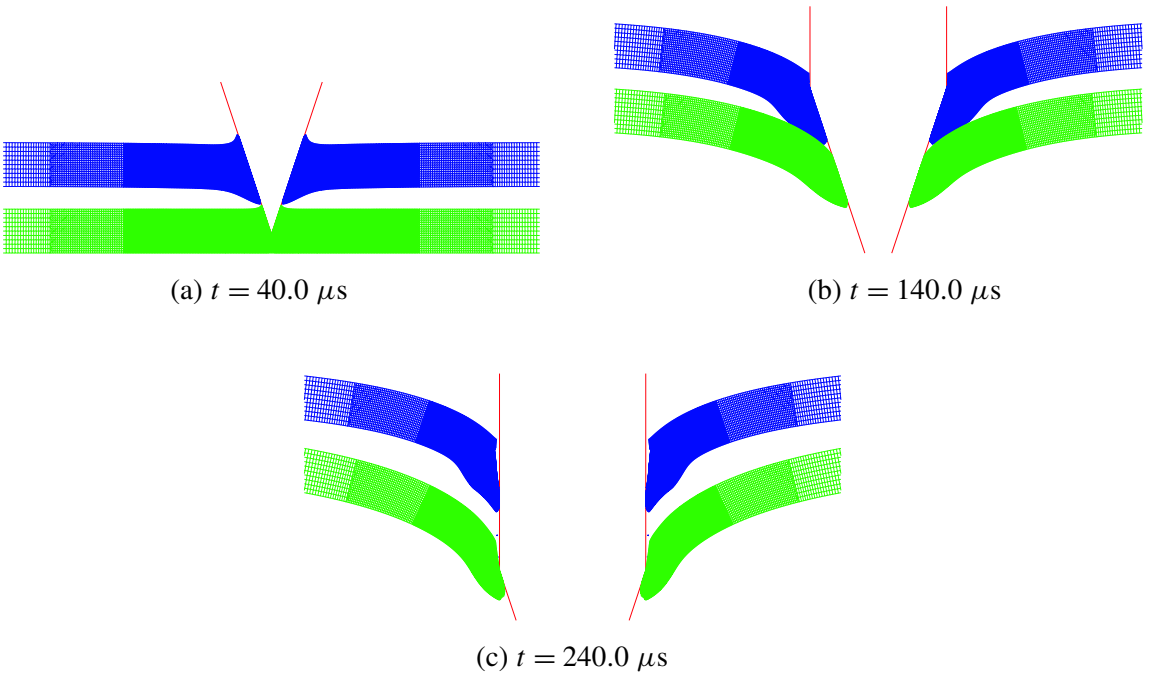


Figure 12. Perforation of double-layered shield with plates spaced impacted by a heavy, conical-nose projectile at $V_0 = 317.9 \text{ m/s}$.

Monolithic plate	Double-layered shield	
	plates in contact	plates spaced
305.9 (1.00)	282.0 (0.922)	280.0 (0.915)

Table 2. Ballistic limits under the impact of a heavy, conical-nose projectile (unit: m/s).

The calculated residual velocities for the double-layered shield with the plates in contact are a little higher than those with the plates spaced. However, the difference is so small as to be indiscernible in Figure 13. The results are again consistent with the experimental observations by Almohandes et al. [1996] and Dey et al. [2007]. It may be concluded, therefore, that an increase in the spacing between the two plates would not considerably improve the protection ability of double-layered shields.

3.3. Light flat-nose projectile. IEDs generate fragments of various configuration and masses. Therefore, in addition to the preceding heavy ones, we use a flat-nose projectile of 10 g mass and diameter $d = 7.6$ mm to represent a light fragment. This striker is close in size to the smallest FSP of 0.30" caliber specified in Military Standard MIL-P-46593A [DoD 1962]. Since the projectile is relatively light, a high impact velocity is required to completely perforate the target. This leads to a different failure mode from shear plugging or tensile tearing.

Figure 14 displays the failure process of the monolithic plate at $V_0 = 600$ m/s. It appears that the materials in the impacted zone beneath the projectile are pushed aside as the projectile moves down. The generated cavity is of a larger diameter on the proximal surface than the projectile. By contrast, at a low impact velocity the cavity is of almost the same diameter through the target thickness, as can be seen, for example, in Figure 5. As the projectile approaches the rear surface of the target, shear plugging becomes the dominating failure mode and a plug of reduced thickness is ejected. It should be pointed out that the reduction in the thickness of the plug does not result from artificial element erosion. Although the remainder of the ligament is broken due to the combined action of tension and shear, ductile hole

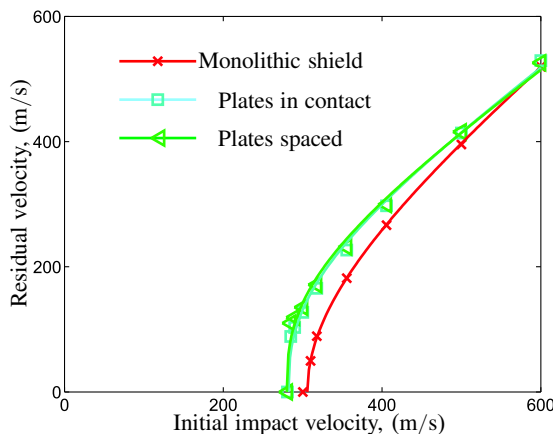


Figure 13. Initial impact velocity vs. residual velocity for three shields impacted by a heavy, conical-nose projectile.

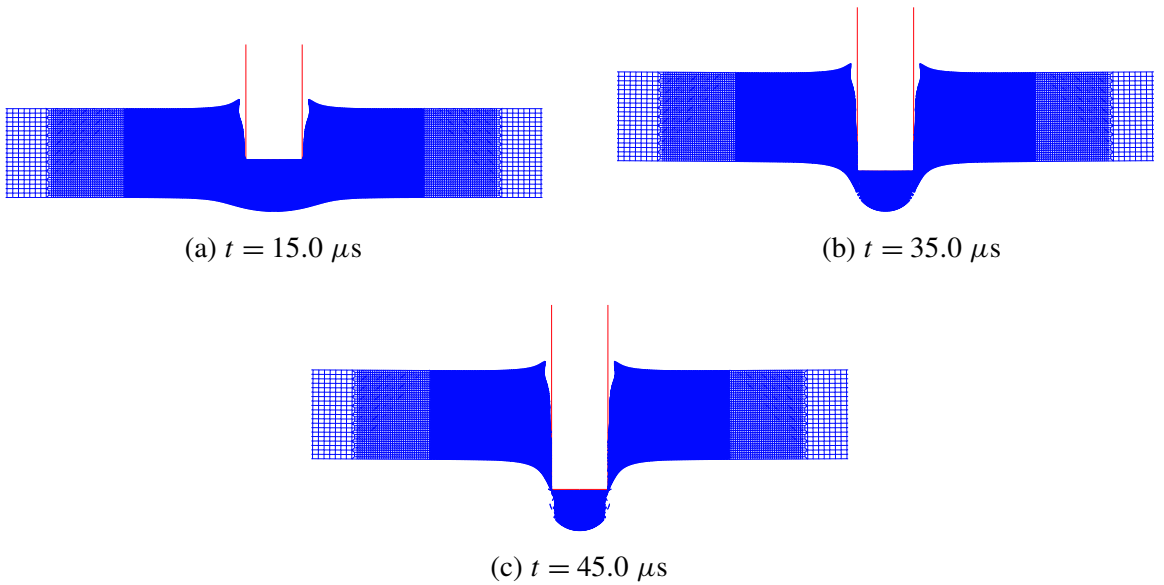


Figure 14. Perforation of monolithic shield impacted by a light, flat-nose projectile at $V_0 = 600.0 \text{ m/s}$.

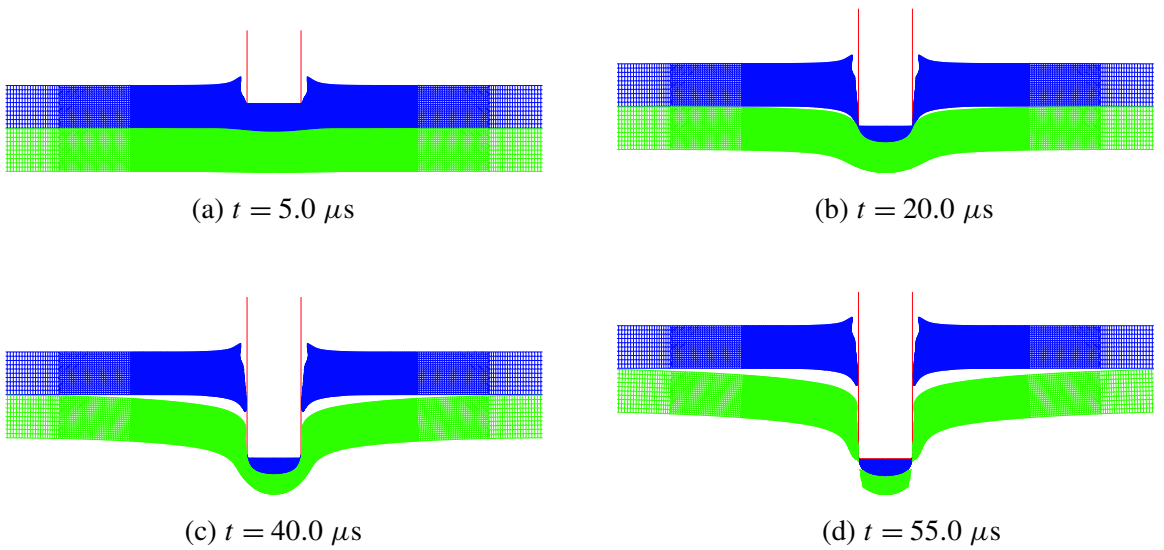


Figure 15. Perforation of double-layered shield with plates in contact impacted by a light, flat-nose projectile at $V_0 = 600.0 \text{ m/s}$.

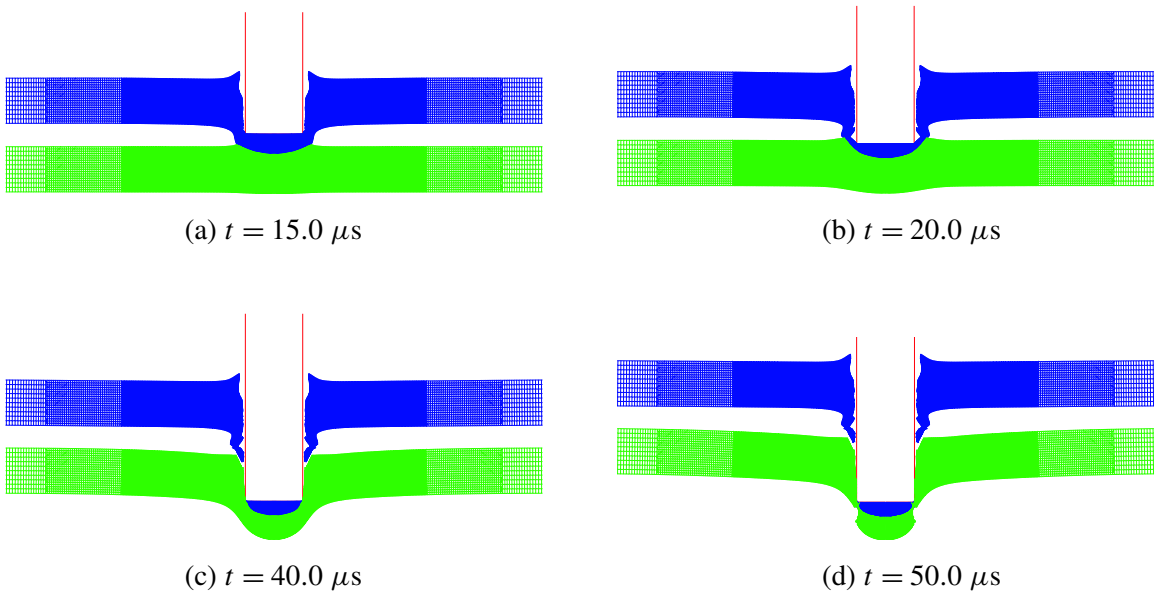


Figure 16. Perforation of double-layered shield with plates spaced impacted by a light, flat-nose projectile at $V_0 = 600.0$ m/s.

enlargement is the predominant failure mechanism. A large part of plastic energy dissipation can be attributed to cavity formation. By contrast, shear plugging is always observed in the monolithic plate under impact by the heavy, flat-nose projectile and the ejected plug is of almost the same thickness as the pretest plate.

A typical fracture process of the double-layered shield with the plates adjacent is given in [Figure 15](#). It can be seen that the upper plate fails mainly by ductile hole enlargement, which is similar to the monolithic shield. The lower plate undergoes a little bending deformation, and necking preceding fracture can be clearly observed. The case with the plates spaced exhibits a similar failure process and pattern; see [Figure 16](#).

Plots of the initial impact velocity versus the residual velocity for the three types of shields are presented in [Figure 17](#). As the impact velocity approaches the ballistic limit, a small advantage of the double-layered shields over the monolithic one becomes clear. The ballistic limit of the double-layered shields is higher by about 7% than that of the monolithic plate; see [Table 3](#) for the detailed information. The increase in the ballistic limit of the double-layer shields can be attributed to the increase in the bending deformation of the lower plate. While the double-layered shield is of the same total thickness as the monolithic one, the elastic bending stiffness of the former is only one quarter of that of the latter.

The predicted ballistic limit of the double-layered shield with the plates spaced is slightly higher than that with the plates in contact. However, the variation in the spacing between the two plates would not be able to considerably improve the protection performance since the failure mode is kept virtually unchanged.

Monolithic plate	Double-layered shield	
	plates in contact	plates spaced
487.4 (1.00)	520.0 4(1.07)	523.0 (1.07)

Table 3. Ballistic limits under the impact of a light, flat-nose projectile (unit: m/s).

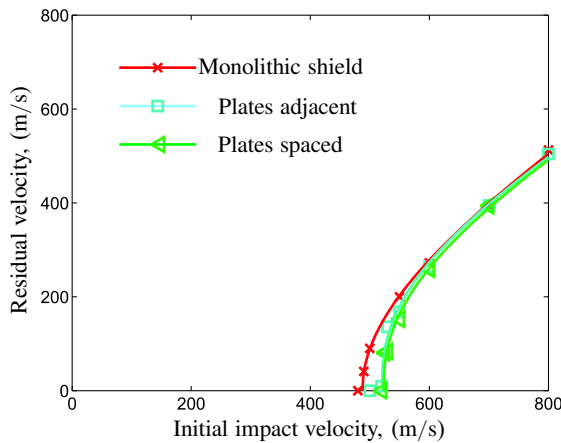


Figure 17. Initial impact velocity vs. residual velocity for three shields impacted by a light, flat-nose projectile.

3.4. Light conical-nose projectile. The 10.0 g projectile can be thought of as a simplification of a standard 7.62 mm hard-core bullet. A real bullet projectile consists of a hard core, a actuator, and a jacket and usually has an ogival nose rather than a conical nose. However, [Dey et al. \[2004\]](#) found from a series of tests that a conical-nose projectile has a very similar perforation capability as that of ogival-nose shape.

Figures 18–20 display the typical perforation processes of the three types of shields at $V_0 = 600.0$ m/s. It appears that all the three metal shields simply fail by ductile hole enlargement. The targets are subjected to little structural deformation, while plastic deformation concentrates in the impacted zone beneath the projectile. This fracture pattern is also observed at all the other impact velocities. Note that this failure mechanism is almost identical to the one in the previous case of the heavy projectile. Hence, for the conical-nose projectile, the implementation of the double layer configuration would not introduce a new failure mode.

Plots of the initial impact velocity versus the residual velocity for the three types of shields are displayed in [Figure 21](#). The corresponding ballistic limits are listed in [Table 4](#). It appears that the double

Monolithic plate	Double-layered shield	
	plates in contact	plates spaced
525.9 (1.000)	524.5 (0.997)	522.54 (0.994)

Table 4. Ballistic limits under impact of a light, conical-nose projectile (unit: m/s).

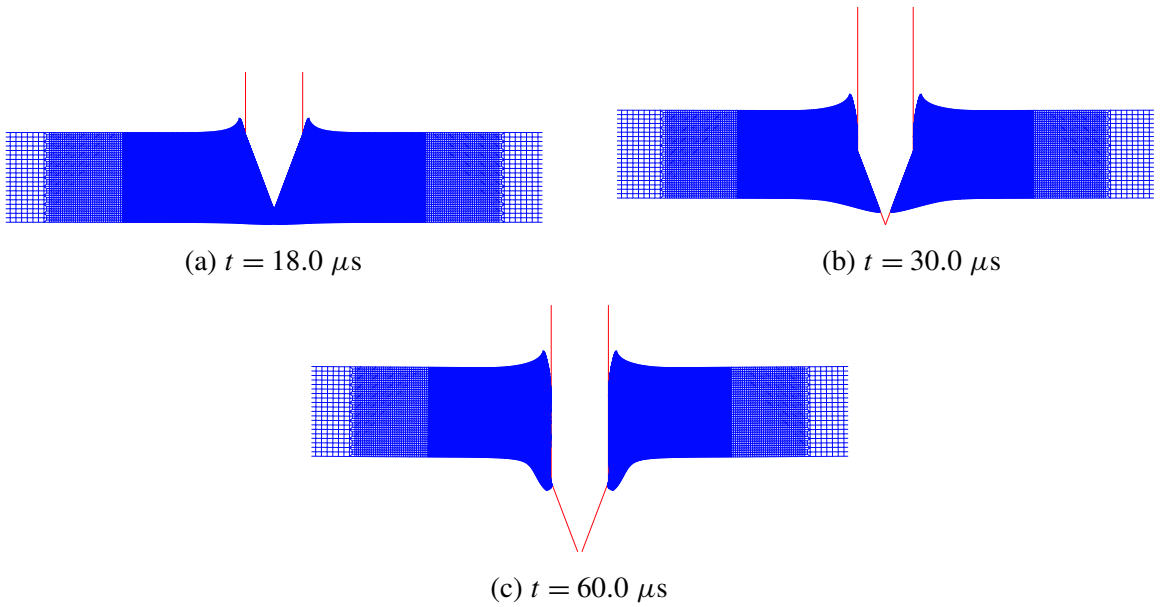


Figure 18. Perforation of monolithic shield impacted by a light, conical-nose projectile at $V_0 = 600.0$ m/s.

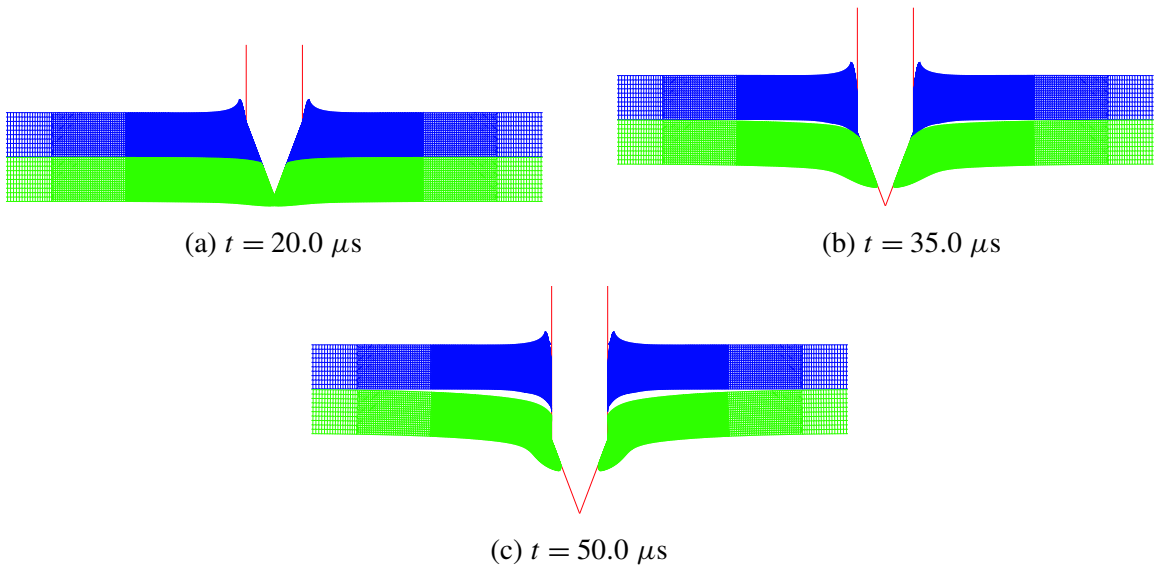


Figure 19. Perforation of double-layered shield with plates in contact impacted by a light, conical-nose projectile at $V_0 = 600.0$ m/s.

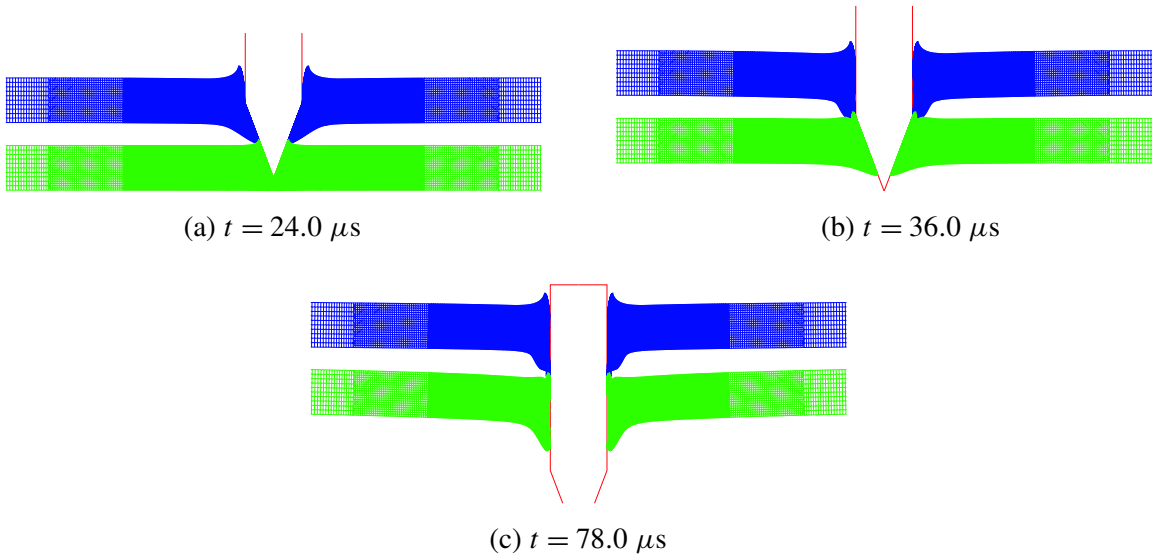


Figure 20. Perforation of double-layered shield with plates spaced impacted by a light, conical-nose projectile at $V_0 = 600.0$ m/s.

layer configuration slightly weakens the ballistic resistance of the shields. However, the difference between the monolithic plate and the double-layered shields is so small that it can be neglected. At the same time, the numerical results indicate that the increase in the spacing between the two plates does not improve the protection performance of the shield.

A few armor piercing experiments were performed on the double-, multilayered shields under impact by the standard 7.62 mm caliber bullet balls [Almohandes et al. 1996; Gupta and Madhu 1997]. They

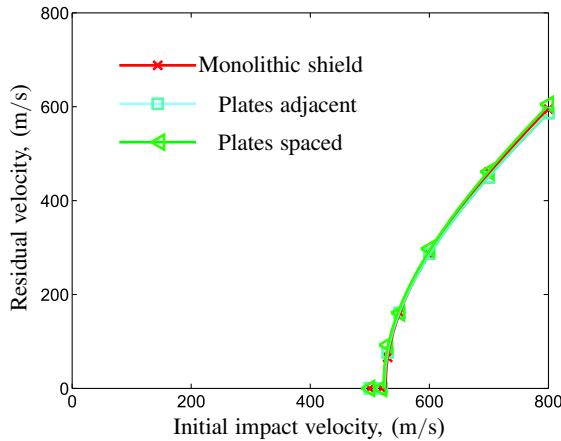


Figure 21. Initial impact velocity vs. residual velocity for three shields impacted by a light, conical-nose projectile.

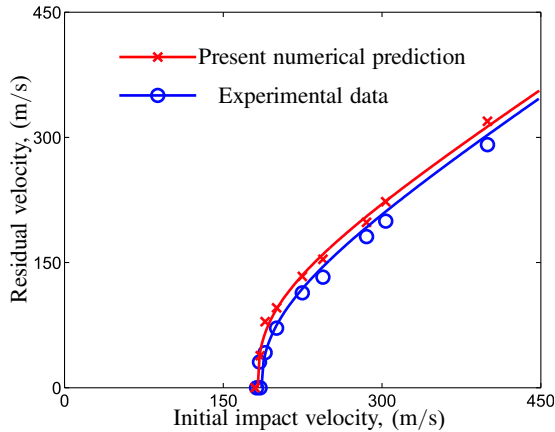


Figure 22. Comparison of residual velocities between numerical prediction and experimental results for monolithic plate impacted by a heavy, flat-nose projectile.

found a slight degradation in the protection behavior of the double-, multilayered shields, compared to the monolithic target of the same total weight. The present numerical prediction qualitatively agrees with those test results.

3.5. Comparison with experimental results. Børvik et al. [2002b; 2002a] performed an extensive experimental and numerical study on the ballistic resistance of a Weldox 460 E steel plate impacted by flat-nose, round-nose, and conical-nose projectiles. Strength and fracture properties of Weldox steel were calibrated by conducting a series of tensile tests on round bars under various strain rates and elevated temperature [Børvik et al. 2001]. The complete experimental results published in the literature provide a solid platform to examine numerical procedures.

For this purpose, the geometry configuration of the projectile-target plate system for the monolithic shield was taken to be identical to the one designed by Børvik et al. [2002b]. This allows the present numerical predictions to be verified by direct comparison to the experimental results.

Figures 22 and 23 display plots of the initial impact velocity versus the residual velocity for the case with the monolithic plate under impact by the heavy flat-nose and the conical-nose projectile, respectively. It appears that the numerical results correlate well with the test data. This validates the correctness of the present finite element procedure.

A number of perforation tests on double-layered plates were performed recently by Dey et al. [2007]. Targets made of Weldox 700 E steel were impacted by a flat-nose and a ogival-nose projectile, respectively, using a gas-gun at subordnance velocities. It was found that the ballistic resistance could be increased by about 30% by using the double layer configuration instead of the monolithic plate in the case with the flat-nose projectile as evidenced in Figure 24. The present numerical finding is closely consistent with this experimental conclusion. Since plasticity and fracture properties of Weldox 700 E steel significantly different from those of Weldox 460 E steel, the experimental results cannot be directly compared with the present numerical work. A detailed description of the experimental procedure and results is presented in a separate publication by Dey et al. [2007].

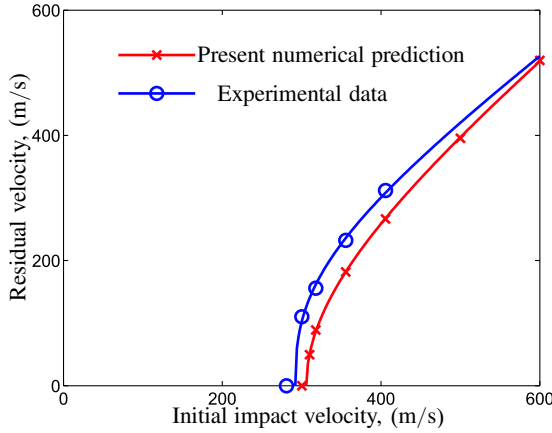


Figure 23. Comparison of residual velocities between numerical prediction and experimental results for monolithic plate impacted by a heavy, conical-nose projectile.

4. Discussion and conclusions

In this work we have examined the effectiveness of the double-layered shield against projectile impact using numerical methods. Four types of projectiles of different mass and nose shape were considered, representing various fragments generated from IEDs. It was found that compared to the monolithic plate, the double layer configuration is able to improve the ballistic limit by 7%–25% for the target under impact by flat-nose projectiles. For conical-nose projectiles the double layer configuration slightly weakens the ballistic resistance. The numerical findings are qualitatively consistent with the experimental results in the open literature. To further verify the findings in the present study, an experimental and numerical program has been carried out at Norwegian University of Science and Technology [Dey et al. 2007].

With the increase in the ballistic limit for the case of a flat-nose projectile, the double layer configuration is able to upgrade the overall protection performance of a target. An armor shield may encounter

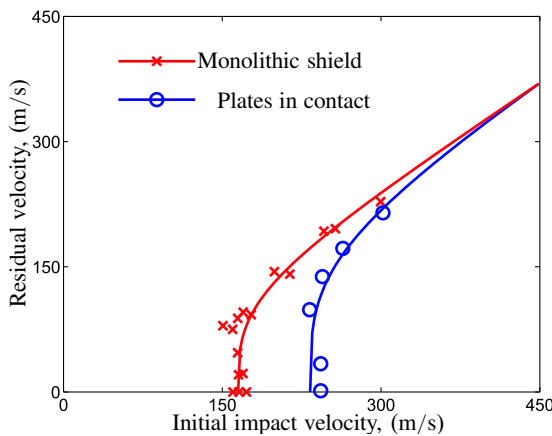


Figure 24. Comparison of experimentally obtained residual velocities between monolithic and double-layered shield [Dey et al. 2007].

the impact of various projectiles. Experimental studies reveal that a projectile of flat-nose is much more detrimental than that of round-nose, conical-nose, or ogival-nose [Børvik et al. 2002b; Dey et al. 2004], that is, a thin or moderately thick target is of the lowest ballistic limit under impact by a flat-nose projectile.

The present numerical investigation indicates that it is not necessary to perfectly bond two layers to enhance the effectiveness of a composite metal shield. The double-layered shield is as effective as, or more effective than, a monolithic plate of the same weight. At the same time, the double layer metal shield would be easily maintained. Partially penetrated/damaged plates can be replaced without changing a whole shield.

This research also indicates that the increase in the spacing between the two plates would not significantly improve the ballistic resistance of the double-layered shields. Actually, the gap decreases the ballistic limit for the case with the conical-nose projectile. Note that by increasing the gap, double-layered shields would occupy more space. However, a systematic parametric study on the effects of the spacing should be further conducted to verify this observation.

In the present study the two plates in the double-layered shield are assumed to be of the same material and thickness. Limited studies indicate that the protection performance of double-layered shields can be further enhanced by placing a thinner plate in front of a thicker plate [Corran et al. 1983b; Corran et al. 1983a]. This conclusion can also be extended to the case with conical-nose projectiles. The experiments conducted by Almohandes et al. [1996] suggest that a double-layered shield consisting of two plates of uneven thickness is of a slightly higher ballistic limit than that of the same thickness. A related question concerns using two different grades of metals with various strengths and ductilities to further increase the ballistic limit of the double-layered shield. This problem is the subject of an ongoing study. The effectiveness of triple-, multilayer configuration also remains to be investigated. For a specific application, these questions can be clarified by conducting an extensive parametric numerical study combined with some experimental validation tests.

References

- [Almohandes et al. 1996] A. A. Almohandes, M. S. Abdel-Kader, and A. M. Eleiche, “Experimental investigation of the ballistic resistance of steel-fiberglass reinforced polyester laminated plates”, *Compos. B Eng.* **27**:5 (1996), 447–458.
- [Bao and Wierzbicki 2005] Y. Bao and T. Wierzbicki, “On the cut-off value of negative triaxiality for fracture”, *Eng. Fract. Mech.* **72**:7 (2005), 1049–1069.
- [Ben-Dor et al. 1998] G. Ben-Dor, A. Dubinsky, and T. Elperin, “On the ballistic resistance of multi-layered targets with air gaps”, *Int. J. Solids Struct.* **35**:23 (1998), 3097–3103.
- [Ben-Dor et al. 2006] G. Ben-Dor, A. Dubinsky, and T. Elperin, “Effect of air gaps on the ballistic resistance of ductile shields perforated by nonconical impactors”, *J. Mech. Mater. Struct.* **1** (2006), 279–299.
- [Børvik et al. 2001] T. Børvik, O. S. Hopperstad, T. Berstad, and M. L. Langseth, “A computational model of viscoplasticity and ductile damage for impact and penetration”, *Eur. J. Mech. A: Solids* **20**:5 (2001), 685–712.

- [Børvik et al. 2002a] T. Børvik, O. S. Hopperstad, T. Berstad, and M. Langseth, “Perforation of 12 mm thick steel plates by 20 mm diameter projectiles with flat, hemispherical and conical noses, II: Numerical simulations”, *Int. J. Impact. Eng.* **27**:1 (2002), 37–64.
- [Børvik et al. 2002b] T. Børvik, M. Langseth, O. S. Hopperstad, and K. A. Malo, “Perforation of 12 mm thick steel plates by 20 mm diameter projectiles with flat, hemispherical and conical noses, I: Experimental study”, *Int. J. Impact. Eng.* **27**:1 (2002), 19–35.
- [Børvik et al. 2003] T. Børvik, O. S. Hopperstad, M. Langseth, and K. A. Malo, “Effects of target thickness in blunt projectile penetration of Weldox 460 E steel plates”, *Int. J. Impact. Eng.* **28**:4 (2003), 413–464.
- [Børvik et al. 2005] T. Børvik, O. S. Hopperstad, S. Dey, E. V. Pizzinato, M. Langseth, and C. Albertini, “Strength and ductility of Weldox 460 E steel at high strain rates, elevated temperatures and various stress triaxialities”, *Eng. Fract. Mech.* **72**:7 (2005), 1071–1087.
- [Børvik et al. 2006] T. Børvik, S. Dey, and A. H. Clausen, “A preliminary study on the perforation resistance of high-strength steel plates”, *J. Phys. (France) IV* **134** (2006), 1053–1059.
- [Corran et al. 1983a] R. S. J. Corran, C. Ruiz, and P. J. Shadbolt, “On the design of containment shields”, *Comput. Struct.* **16**:1–4 (1983), 563–572.
- [Corran et al. 1983b] R. S. J. Corran, P. J. Shadbolt, and C. Ruiz, “Impact loading of plates: An experimental investigation”, *Int. J. Impact. Eng.* **1**:1 (1983), 3–22.
- [Dey et al. 2004] S. Dey, T. Børvik, O. S. Hopperstad, J. R. Leinum, and M. Langseth, “The effect of target strength on the perforation of steel plates using three different projectile nose shapes”, *Int. J. Impact. Eng.* **30**:8–9 (2004), 1005–1038.
- [Dey et al. 2007] S. Dey, T. Børvik, X. Teng, T. Wierzbicki, and O. S. Hopperstad, “On the ballistic resistance of double-layered steel plates: An experimental and numerical investigation”, *Int. J. Solids Struct.* (2007). In press.
- [DoD 1962] DoD, “Projectile, calibers 0.22, 0.30, 0.50, and 20 mm fragment-simulating”, Military Specification MIL-P-46593A (ORD), Department of Defense, Washington, DC, October 1962.
- [Elek et al. 2005] P. Elek, S. Jaramaz, and D. Micković, “Modeling of perforation of plates and multi-layered metallic targets”, *Int. J. Solids Struct.* **42**:3–4 (2005), 1209–1224.
- [Gupta and Madhu 1997] N. K. Gupta and V. Madhu, “An experimental study of normal and oblique impact of hard-core projectile on single and layered plates”, *Int. J. Impact. Eng.* **19**:5–6 (1997), 395–414.
- [Johnson and Cook 1983] G. R. Johnson and W. H. Cook, “A constitutive model and data for metals subjected to large strains, high strain rates and high temperatures”, pp. 541–547 in *Proceedings of the 7th International Symposium on Ballistics* (Hague), American Defense Preparedness Association, 1983.
- [Johnson and Cook 1985] G. R. Johnson and W. H. Cook, “Fracture characteristics of three metals subjected to various strains, strain rates, temperatures and pressures”, *Eng. Fract. Mech.* **21**:1 (1985), 31–48.
- [Liang et al. 2005] C. C. Liang, M. F. Yang, P. W. Wu, and T. L. Teng, “Resistant performance of perforation of multi-layered targets using an estimation procedure with marine application”, *Ocean Eng.* **32**:3–4 (2005), 441–468.
- [Liss et al. 1983] J. Liss, W. Goldsmith, and J. M. Kelly, “A phenomenological penetration model of plates”, *Int. J. Impact. Eng.* **1**:4 (1983), 321–341.
- [Marom and Bodner 1979] I. Marom and S. R. Bodner, “Projectile perforation of multilayered beams”, *Int. J. Mech. Sci.* **21**:8 (1979), 489–504.
- [Radin and Goldsmith 1988] J. Radin and W. Goldsmith, “Normal projectile penetration and perforation of layered targets”, *Int. J. Impact. Eng.* **7**:2 (1988), 229–259.
- [Teng and Wierzbicki 2005a] X. Teng and T. Wierzbicki, “Numerical study on crack propagation in high velocity perforation”, *Comput. Struct.* **83**:12–13 (2005), 989–1004.
- [Teng and Wierzbicki 2005b] X. Teng and T. Wierzbicki, “Transition of failure modes in round-nosed mass-to-beam impact”, *Eur. J. Mech. A: Solids* **24**:5 (2005), 857–876.

[Teng et al. 2005] X. Teng, T. Wierzbicki, S. Hiermaier, and I. Rohr, “Numerical prediction of fracture in the Taylor test”, *Int. J. Solids Struct.* **42**:9–10 (2005), 2929–2948.

Received 2 Jan 2007. Accepted 12 Mar 2007.

XIAOQING TENG: xteng@alum.mit.edu

Impact and Crashworthiness Lab, Massachusetts Institute of Technology, 77 Massachusetts Avenue, Room 5-218, Cambridge, MA 02139, United States

SUMITA DEY: Sumita.Dey@forsvarsbygg.no

Structural Impact Laboratory, Norwegian University of Science and Technology, Rich. Birkelands vei 1A, NO-7491, Trondheim, Norway

TORE BØRVIK: tore.borvik@ntnu.no

Structural Impact Laboratory, Norwegian University of Science and Technology, Rich. Birkelands vei 1A, NO-7491, Trondheim, Norway

TOMASZ WIERZBICKI: wierz@mit.edu

Impact and Crashworthiness Lab, Massachusetts Institute of Technology, 77 Mass Avenue, Room 5-218, Cambridge, MA 02139, United States